Polarization effects in the elastic $e\vec{p} \to \vec{e}p$ and $\vec{e}\,\vec{p} \to ep$ processes in the case of parallel spins

M. V. Galynskii[*]
Joint Institute for Power and Nuclear Research—Sosny, National Academy of Sciences of Belarus, 220109 Minsk, Belarus

V. V. Bytev[†]
Joint Institute for Nuclear Research—Dubna, Russia

V. M. Galynsky[‡]
Belarusian State University, Minsk 220030, Belarus

(Received 6 August 2024; accepted 11 October 2024; published 22 November 2024)

In the one-photon exchange approximation, we analyze polarization effects in the elastic $\vec{e}\,\vec{p} \to ep$ and $e\vec{p} \to \vec{e}p$ processes in the case when the spin quantization axes of a target proton at rest and an incident or scattered electron are parallel. To do this, in the kinematics of the SANE Collaboration experiment [A. Liyanage *et al.*, Phys. Rev. C **101**, 035206 (2020)] using the J. Kelly [Phys. Rev. C **70**, 068202 (2004)] and I. Qattan *et al.* [Phys. Rev. C **91**, 065203 (2015)] parametrizations for the Sachs form-factor ratio $R \equiv \mu_p G_E/G_M$, a numerical analysis was carried out of the dependence of the longitudinal polarization degree transferred to the scattered electron in the $e\vec{p} \to \vec{e}p$ process and double-spin asymmetry in the $\vec{e}\,\vec{p} \to ep$ process on the square of the momentum transferred to the proton, as well as on the scattering angle of the electron. It is established that the difference in the longitudinal polarization degree of the scattered electron in the $e\vec{p} \to \vec{e}p$ process in the cases of conservation and violation of the scaling of the Sachs form factors can reach 70%. This fact can be used to set up polarization experiments of a new type to measure the ratio R. For double-spin asymmetry in the $\vec{e}\,\vec{p} \to ep$ process, the corresponding difference does not exceed 2.32%. This fact means that it is not sensitive to the effects of the Sachs form-factor scaling violation and could be used as a test for the $R \approx 1$ equality.

DOI: 10.1103/PhysRevD.110.096017

I. INTRODUCTION

Experiments on the study of electric G_E and magnetic G_M proton form factors, the so-called Sachs form factors (SFFs), have been performed since the mid-1950s in the elastic process of electron-proton scattering [1]. In the case of unpolarized electrons and protons, all experimental data on the behavior of the SFFs were obtained with the help of the Rosenbluth technique (RT) based on the Rosenbluth formula for the differential cross section for the $ep \to ep$ process in the rest frame of the initial proton [2]—that is,

$$\frac{d\sigma}{d\Omega_e} = \frac{\alpha^2 E_2 \cos^2(\theta_e/2)}{4E_1^3 \sin^4(\theta_e/2)} \frac{1}{1+\tau_p}\left(G_E^2 + \frac{\tau_p}{\varepsilon} G_M^2\right). \quad (1)$$

Here, $\tau_p = Q^2/4m^2$; $Q^2 = 4E_1E_2\sin^2(\theta_e/2)$ is the square of the 4-momentum transferred to the proton; m is the mass of the proton; E_1, E_2 are the energies of the initial and final electrons; θ_e is the electron scattering angle; $\varepsilon = [1 + 2(1+\tau_p)\tan^2(\theta_e/2)]^{-1}$ is the degree of linear (transverse) polarization of the virtual photon [3–6]; and $\alpha = 1/137$ is the fine structure constant. Expression (1) was obtained in the one-photon exchange (OPE) approximation, and the electron mass was set to zero.

With the help of the RT, the dipole dependence of the SFFs on the momentum transferred to the proton square Q^2 in the region $Q^2 \leq 6\ \mathrm{GeV}^2$ was established (see Ref. [7] for an exhaustive review). As it turned out, these measurements indicate approximate form-factor scaling—i.e., $\mu_p G_E/G_M \approx 1$, where $\mu_p = 2.79$ is the magnetic moment of the proton.

[*]Contact author: galynski@sosny.bas-net.by
[†]Contact author: bvv@jinr.ru
[‡]Contact author: galynsky@bsu.by

Akhiezer and Rekalo [4] proposed a method for measuring the $R \equiv \mu_p G_E/G_M$ ratio based on the phenomenon of polarization transfer from the initial electron to the final proton in the $\vec{e}p \to e\vec{p}$ process (later, this method was generalized in Ref. [8]). Precision JLab experiments [9–11], using this method, found a fairly rapid decrease in the ratio of R with an increase in Q^2, which indicates the violation of the dipole dependence over the transferred momentum square Q^2. In the range $0.4\ \mathrm{GeV}^2 \le Q^2 \le 5.6\ \mathrm{GeV}^2$, as it turned out, this decrease is linear. Next, more accurate measurements of the ratio R carried out in [12–16] in a wide area in Q^2 up to $8.5\ \mathrm{GeV}^2$, using both the Akhiezer-Rekalo (AR) method [4] and the RT [16], only confirmed the discrepancy of the results.

In the SANE Collaboration experiment [17], the values of R have been measured for the elastic $\vec{e}\,\vec{p} \to ep$ process by the third method [18] using double-spin asymmetry for target spin orientation aligned nearly perpendicular to the beam momentum direction in the case when the electron beam and the proton target are partially polarized. The degree of polarization of the proton target was $P_t = (70 \pm 5)\%$. The experiment was performed at two electron beam energies E_1, 4.725 and 5.895 GeV, and two Q^2 values, $2.06\ \mathrm{GeV}^2$ and $5.66\ \mathrm{GeV}^2$. The extracted values of R in [17] are consistent with the results in Refs. [9–15].

Currently, the most precise measurements of the proton FFs at low momentum transfer, and of its charge and magnetic radii, were performed by the A1 Collaboration at MAMI, Mainz [19–21]. Cross sections were measured at 1422 kinematic settings, covering a Q^2 range from 0.004 to $1.0\ \mathrm{GeV}^2$ with an average point-to-point systematic error of 0.37% [19–21]. With this large dataset, the authors extracted G_E and G_M by a direct fit of form-factor models to cross-section data, rather than the traditional Rosenbluth separation technique. The results of the fits reconcile with a classic Rosenbluth separation within error estimations.

Thus, while the Rosenbluth data are compatible with the scaling relation prediction, polarized experiments yield data with a linear, downward trend. The most commonly proposed explanation for this discrepancy are "hard" two-photon exchange (TPE) contributions beyond the standard radiative corrections to OPE [22–24]. Note that the recent TPE experiments [25–29] show little evidence for significant contributions beyond OPE up to $Q^2 \approx 2.3\ \mathrm{GeV}^2$ [30]. To determine whether "hard" TPE contributions could explain the form-factor discrepancy, one needs new measurements at higher Q^2.

The presence of a polarized proton target with a high degree of polarization motivates the study of polarization effects (including double-spin correlations) in the processes such as $e\vec{p} \to e\vec{p}$, $e\vec{p} \to \vec{e}p$, $\vec{e}\,\vec{p} \to ep$ in order to find possibilities for setting up polarization experiments of a new type for measuring the elastic proton form factors.

In Refs. [31–36], in the OPE approximation, polarization effects in the elastic $e\vec{p} \to e\vec{p}$ process were investigated in the case when the spins of the initial and of the detected recoil proton are parallel—i.e., when a proton is scattered in the direction of the spin quantization axis of the rest proton target. To do this, in the kinematics of the SANE Collaboration experiment [17] on measuring double-spin asymmetry in the $\vec{e}\,\vec{p} \to ep$ process, using the Kelly [37] and Qattan [38] parametrizations for the R ratio, a numerical analysis was carried out of the dependence of the longitudinal polarization degree of the scattered proton on the square of the momentum transferred to the proton, as well as on the scattering angles of the electron and proton. In this case, a noticeable sensitivity of the polarization transferred to the proton to the type of dependence of the ratio R on Q^2 was established, and it was also shown that the violation of the scaling of the SFFs leads to a significant increase in the magnitude of the polarization transfer to the proton, as compared to the case of the dipole dependence. Thus, in Refs. [31–36], the fourth method for measuring the ratio of R was proposed, based on the transfer of polarization from the initial proton to the final one in the $e\vec{p} \to e\vec{p}$ process in the case where their spins are parallel. This method also works in the TPE approximation and allows us to measure the squares of the modules of generalized SFFs [33].

Note that Akhiezer and Rekalo (see [5], pp. 211–215) also performed a general calculation of the $e\vec{p} \to e\vec{p}$ cross section in the Breit system for partially polarized initial and final protons. However, they analyzed this cross section in [5] by analogy with [4] and overlooked a more interesting case, which was discussed in Refs. [31–36].

In our recent short paper [39], the fifth method of measuring the ratio R was proposed, based on the transfer of polarization from the initial proton to the final electron in the elastic $e\vec{p} \to \vec{e}p$ process in the case where the spin quantization axes of the resting proton target and the scattered electron are parallel—i.e., when the electron is scattered in the direction of the spin quantization axis of the resting proton target.

In Refs. [34–36,39], we utilize two commonly used parametrizations of the SFFs. First, Kelly parametrization [37] (and similar ones [40–42]) is based on a mix of cross section and polarization data, but without the TPE corrections. Second, Qattan parametrization [38] (see also [43]) includes phenomenological TPE corrections extracted from the difference between Rosenbluth and polarization measurements. Although there exist more modern and sophisticated fits to proton data [44,45], we restricted our calculations to these two, as it shows negligible differences in our results from different types of parametrizations.

The aim of this article is to give a more detailed view of the results of the work [39], as well as to investigate the double-spin asymmetry in the $\vec{e}\,\vec{p} \to ep$ process in the case

of parallel spins of the initial electron and proton. To do this, in the kinematics of the SANE Collaboration experiment [17] using the Kelly [37] and Qattan [38] parametrizations for the SFF ratio R, a numerical analysis was carried out of the dependence of the longitudinal polarization degree transferred to the scattered electron in the $e\vec{p} \to \vec{e}p$ process and the double-spin asymmetry in the $\vec{e}\,\vec{p} \to ep$ process on the square of the momentum transferred to the proton, as well as on the scattering angle of the electron.

II. HELICITY AND DIAGONAL SPIN BASES

The spin 4-vector $s = (s_0, \boldsymbol{s})$ of the fermion with 4-momentum p $(p^2 = m^2)$ satisfying the conditions of orthogonality and normalization is given by

$$s = (s_0, \boldsymbol{s}), \qquad s_0 = \frac{\boldsymbol{cp}}{m}, \qquad \boldsymbol{s} = \boldsymbol{c} + \frac{(\boldsymbol{cp})\boldsymbol{p}}{m(p_0 + m)}, \tag{2}$$

where $\boldsymbol{c}$ is the spin quantization axis $(\boldsymbol{c}^2 = 1)$.

The expressions in Eq. (2) allow us to determine the spin 4-vector $s = (s_0, \boldsymbol{s})$ by a given 4-momentum $p = (p_0, \boldsymbol{p})$ and 3-vector $\boldsymbol{c}$. On the contrary, if the 4-vector s is known, then the spin quantization axis $\boldsymbol{c}$ is given by

$$\boldsymbol{c} = \boldsymbol{s} - \frac{s_0}{p_0 + m}\boldsymbol{p}; \tag{3}$$

i.e., the vectors $\boldsymbol{c}$ and s at a given p uniquely define each other.

For the calculation of polarization effects in high-energy physics processes, one usually utilizes helicity basis, introduced by Jacob and Wick [46], in which the spin quantization axis $\boldsymbol{c}$ is directed along the momentum of the particle

$$\boldsymbol{c} = \boldsymbol{n} = p/|\boldsymbol{p}|,$$

while the spin 4-vector s (2) reads

$$s = (s_0, \boldsymbol{s}) = (|\boldsymbol{v}|, v_0\boldsymbol{n}),$$

where v_0 and $\boldsymbol{v}$ are the time and space components of the 4-velocity vector $v = p/m$ $(v^2 = 1)$.

The popularity of the helicity basis is primarily due to the simplicity of the physical interpretation of the helicity definition (projection of the spin in the direction of the particle momentum), and its emphasis on the center-of-mass system. At the same time, studying the helicities of moving particles is analogous to the study of the spins of particles at rest [47,48]. However, there are several important factors which prevent helicity from playing the dominant role in describing the spin projection of particles. One is that helicity is not a particle characteristic that is invariant under the Lorentz transformation [47–50]. In interpreting the dynamics of spin interaction, the amplitudes of scattering processes with and without changing the sign of the particle helicity are often referred to as amplitudes with and without a spin flip. However, since the particle momentum is changed by the interaction, it is clear that such a classification is very arbitrary. Both types of amplitudes actually describe a process with a change in the particle spin state.

In general, for a system of two particles with different 4-momenta $q_1 = (q_{10}, \boldsymbol{q}_1)$ (before interaction) and $q_2 = (q_{20}, \boldsymbol{q}_2)$ (after interaction), the possibility of the quantization of spins in one common direction, including the case where particles have different masses, is determined by the three-dimensional vector given by [47]

$$\boldsymbol{a} = \boldsymbol{q}_2/q_{20} - \boldsymbol{q}_1/q_{10}. \tag{4}$$

Since the common spin quantization axis [Eq. (4)] defines the spin basis apart from the helicity basis and is the difference of two three-dimensional vectors, the geometric image of which is the diagonal of a parallelogram, it is natural to call it the diagonal spin basis (DSB). For the first time, in a four-dimensional covariant form, the DSB was constructed in Ref. [51] in the process

$$e(p_1) + p(q_1, s_{p_1}) \to e(p_2) + p(q_2, s_{p_2}). \tag{5}$$

In it, the spin 4-vectors of the initial and final protons s_{p_1} and s_{p_2} are expressed in terms of their 4-momenta q_1 and q_2 $(q_1^2 = q_2^2 = m^2)$ [51]:

$$s_{p_1} = \frac{m^2 q_2 - (q_1 q_2) q_1}{m\sqrt{(q_1 q_2)^2 - m^4}},$$
$$s_{p_2} = \frac{(q_1 q_2) q_2 - m^2 q_1}{m\sqrt{(q_1 q_2)^2 - m^4}}. \tag{6}$$

In the laboratory frame (LF), where the initial proton rests, $q_1 = (m, \boldsymbol{0})$, the spin 4-vectors [Eq. (6)] read

$$s_{p_1} = (0, \boldsymbol{n}_2), \qquad s_{p_2} = (|\boldsymbol{v}_2|, v_{20}\boldsymbol{n}_2), \tag{7}$$

where $\boldsymbol{n}_2 = \boldsymbol{q}_2/|\boldsymbol{q}_2|$, $v_2 = (v_{20}, \boldsymbol{v}_2) = q_2/m$ is the velocity vector of the final proton, $v_2^2 = 1$.

Using the explicit form of the spin 4-vectors in Eq. (7) and formulas (3) or (4), it is easy to verify that the spin quantization axes of the initial and final proton in the LF coincide with the direction of the final proton momentum:

$$\boldsymbol{c} = \boldsymbol{c}_{p_1} = \boldsymbol{c}_{p_2} = \boldsymbol{n}_2 = q_2/|\boldsymbol{q}_2|. \tag{8}$$

In the ultrarelativistic limit, when the masses of protons can be neglected—i.e. at $q_{10}, q_{20} \gg m$—the spin 4-vectors s_{p_1} and s_{p_2} [Eq. (6)] read

$$s_{p_1} = -\frac{q_1}{m}, \qquad s_{p_2} = \frac{q_2}{m}. \tag{9}$$

Let us turn to the consideration of the electron-proton scattering $e\vec{p} \to \vec{e}p$ process in the case where the initial proton and the final electron are polarized:

$$e(p_1) + p(q_1, s_{p_1}) \to e(p_2, s_{e_2}) + p(q_2), \tag{10}$$

where p_1, p_2 are the 4-momenta of the initial and final electrons ($p_1^2 = p_2^2 = m_0^2$).

For the process under consideration [Eq. (10)], we define the common spin quantization axis $\boldsymbol{a}$ and the spin 4-vectors of the initial proton and the final electron, s_{p_1} and s_{e_2}, as follows:

$$\boldsymbol{a} = \boldsymbol{p}_2/p_{20} - \boldsymbol{q}_1/q_{10}, \tag{11}$$

$$s_{p_1} = \frac{m^2 p_2 - (q_1 p_2) q_1}{m\sqrt{(q_1 p_2)^2 - m^2 m_0^2}},$$
$$s_{e_2} = \frac{(q_1 p_2) p_2 - m_0^2 q_1}{m_0\sqrt{(q_1 p_2)^2 - m^2 m_0^2}}. \tag{12}$$

In the LF, the spin 4-vectors [Eq. (12)] read

$$s_{p_1} = (0, \boldsymbol{n}_{e_2}), \qquad s_{e_2} = (|\boldsymbol{v}_{\boldsymbol{e_2}}|, v_{e_{20}}\boldsymbol{n}_{\boldsymbol{e_2}}), \tag{13}$$

where $\boldsymbol{n}_{e_2} = \boldsymbol{p_2}/|\boldsymbol{p}_2|$, $v_{e_2} = (v_{e_{20}}, \boldsymbol{v}_{\boldsymbol{e_2}}) = p_2/m_0$ is the velocity of the final electron, and $v_{e_2}^2 = 1$.

Using the explicit form of the spin 4-vectors in Eq. (13) and formulas (3) or (11), it is easy to verify that the spin quantization axes of the initial proton $\boldsymbol{c}_{p_1}$ and the final electron $\boldsymbol{c}_{e_2}$ in the LF coincide with the direction of the final electron momentum:

$$\boldsymbol{c} = \boldsymbol{c}_{p_1} = \boldsymbol{c}_{e_2} = \boldsymbol{n}_{e_2} = \boldsymbol{p_2}/|\boldsymbol{p}_2|. \tag{14}$$

In the ultrarelativistic limit, when the electron mass can be neglected—i.e., at $p_{10}, p_{20} \gg m_0$—the spin 4-vectors [Eq. (12)] read

$$s_{p_1} = \frac{m^2 p_2 - (q_1 p_2) q_1}{m(q_1 p_2)}, \qquad s_{e_2} = \frac{p_2}{m_0}. \tag{15}$$

Similarly, in the case where the initial electron and proton are polarized in the ep scattering process,

$$e(p_1, s_{e_1}) + p(q_1, s_{p_1}) \to e(p_2) + p(q_2), \tag{16}$$

the common spin quantization axis $\boldsymbol{a}$ and spin 4-vectors of the initial electron and the proton s_{e_1} and s_{p_1} are defined as follows:

$$\boldsymbol{a} = \boldsymbol{p}_1/p_{10} - \boldsymbol{q}_1/q_{10}, \tag{17}$$

$$s_{e_1} = \frac{(q_1 p_1) p_1 - m_0^2 q_1}{m_0\sqrt{(q_1 p_1)^2 - m^2 m_0^2}},$$
$$s_{p_1} = \frac{m^2 p_1 - (q_1 p_1) q_1}{m\sqrt{(q_1 p_1)^2 - m^2 m_0^2}}. \tag{18}$$

Again, in the LF, the spin 4-vectors [Eq. (18)] read

$$s_{p_1} = (0, \boldsymbol{n}_{e_1}), \qquad s_{e_1} = (|\boldsymbol{v}_{\boldsymbol{e_1}}|, v_{e_{10}}\boldsymbol{n}_{\boldsymbol{e_1}}), \tag{19}$$

where $\boldsymbol{n}_{e_1} = \boldsymbol{p_1}/|\boldsymbol{p}_1|$, $v_{e_1} = (v_{e_{10}}, \boldsymbol{v}_{\boldsymbol{e_1}}) = p_1/m_0$ is the velocity of the initial electron, and $v_{e_1}^2 = 1$.

Using the explicit form of the spin 4-vectors in Eq. (19) and formulas (3) or (17), it is easy to verify that the spin quantization axes of the initial proton $\boldsymbol{c}_{p_1}$ and electron $\boldsymbol{c}_{e_1}$ in the LF coincide with the direction of the initial electron momentum:

$$\boldsymbol{c} = \boldsymbol{c}_{e_1} = \boldsymbol{c}_{p_1} = \boldsymbol{n}_{e_1} = \boldsymbol{p_1}/|\boldsymbol{p}_1|. \tag{20}$$

In the ultrarelativistic limit, when the electron mass can be neglected—i.e., at $p_{10}, p_{20} \gg m_0$—the spin 4-vectors [Eq. (18)] read

$$s_{e_1} = \frac{p_1}{m_0}, \qquad s_{p_1} = \frac{m^2 p_1 - (q_1 p_1) q_1}{m(q_1 p_1)}. \tag{21}$$

Thus, in this section, three DSBs corresponding to the $e\vec{p} \to e\vec{p}$, $e\vec{p} \to \vec{e}p$, and $\vec{e}\,\vec{p} \to ep$ processes are built, of which the last two are considered here for the first time.

The fundamental fact that the Lorentz little group common to a system of two particles with different momenta is realized in the DSB leads to a number of remarkable consequences. First, in this basis, particles before and after interaction in the scattering channel have common spin operators [51,52], which allows one to covariantly separate interactions with and without changing of the spin states of the particles involved in the reaction, making it possible to trace the dynamics of the spin interaction. Second, in the DSB, the mathematical structure of the amplitudes is maximally simplified owing to the coincidence of the particle spin operators, the separation of Wigner rotations from the amplitudes [51,52], and the decrease in the number of independent scalar products of 4-vectors that characterize the reaction. Third, in the DSB, the spin states of massless particles coincide up to the sign with the helicity states; see Eq. (9).

III. KINEMATICS AND VARIABLES USED

The differential cross sections of the processes (5), (10), and (16) calculated in the DSB can in principle contain only dot products of the particles' 4-momenta $p_i p_j$, $p_i q_j$, $q_i q_j$ $(i, j = 1, 2)$ involved in reactions. A further significant simplification of expressions can be achieved by moving

from the 4-vectors p_i, q_i to the 4-vectors $p_\pm = p_2 \pm p_1, q_\pm = q_2 \pm q_1$. These satisfy the orthogonal conditions $p_\pm p_\mp = q_\pm q_\mp = p_\pm q_\mp = 0$ and the following simple relations:

$$p_+^2 + p_-^2 = 4m_0^2, \qquad q_+^2 + q_-^2 = 4m^2,$$
$$q_+^2 = 4m^2(1+\tau_p), \qquad \tau_p = -q_-^2/4m^2. \tag{22}$$

In terms of $p_\pm$, $q_\pm$ the 4-vectors of p_i, q_j are

$$p_1 = (p_+ - p_-)/2, \qquad p_2 = (p_+ + p_-)/2,$$
$$q_1 = (q_+ - q_-)/2, \qquad q_2 = (q_+ + q_-)/2.$$

Let us introduce the orthonormal vector basis (tetrad) b_A $(A = 0, 1, 2, 3)$:

$$b_0 = \frac{q_+}{\sqrt{q_+^2}}, \qquad b_3 = \frac{q_-}{\sqrt{-q_-^2}},$$
$$(b_2)_\mu = \varepsilon_{\mu\nu\kappa\sigma} q_1^\nu q_2^\kappa r^\sigma/\rho, \qquad (b_1)_\mu = \varepsilon_{\mu\nu\kappa\sigma} b_0^\nu b_3^\kappa b_2^\sigma, \tag{23}$$

where $\varepsilon_{\mu\nu\kappa\sigma}$ is the Levi-Civita tensor ($\varepsilon_{1230} = 1$), r is the 4-momentum of the particle involved in the reaction which is different from q_1 and q_2, and ρ is determined from the normalization conditions

$$b_0^2 = -b_1^2 = -b_2^2 = -b_3^2 = 1.$$

The completeness relation is valid for the tetrad of the 4-vectors b_A [Eq. (23)]:

$$b_{0\mu} b_{0\nu} - b_{1\mu} b_{1\nu} - b_{2\mu} b_{2\nu} - b_{3\mu} b_{3\nu} = g_{\mu\nu}, \tag{24}$$

where $g_{\mu\nu}$ is the metric tensor in the Minkowski space, which is naturally divided into the sum of the longitudinal and transverse parts:

$$g_{\mu\nu} = g_{\mu\nu}^{\parallel} + g_{\mu\nu}^{\perp},$$
$$g_{\mu\nu}^{\parallel} = b_{0\mu} b_{0\nu} - b_{3\mu} b_{3\nu},$$
$$g_{\mu\nu}^{\perp} = -b_{1\mu} b_{1\nu} - b_{2\mu} b_{2\nu}.$$

For the transverse part of the metric tensor, we have

$$g_{\mu\nu}^{\perp} = g_{\mu\nu} - g_{\mu\nu}^{\parallel}.$$

In terms of $(q_\pm)_\mu$, $(q_\pm)_\nu$, the tensor $g_{\mu\nu}^{\perp}$ has the form

$$g_{\mu\nu}^{\perp} = g_{\mu\nu} - \frac{(q_+)_\mu (q_+)_\nu}{q_+^2} + \frac{(q_-)_\mu (q_-)_\nu}{-q_-^2}. \tag{25}$$

For calculations, we also use the Mandelstam variables

$$s = (p_1 + q_1)^2, \qquad t = (q_2 - q_1)^2, \qquad u = (q_2 - p_1)^2 \tag{26}$$

with the standard connection equation

$$s + t + u = 2m_0^2 + 2m^2.$$

By reversing the relation in Eq. (26), for scalar products in terms of s, t, u, we have

$$2p_1q_1 = 2p_2q_2 = s - m_0^2 - m^2,$$
$$2p_1q_2 = 2p_2q_1 = m_0^2 + m^2 - u,$$
$$2p_1p_2 = 2m_0^2 - t, \qquad p_+q_+ = s - u,$$
$$2q_1q_2 = 2m^2 - t, \qquad q_+^2 = 4m^2 - t. \tag{27}$$

A. Ultrarelativistic limit

In the ultrarelativistic limit, when the mass of an electron can be neglected, for the Mandelstam variables in the LF, we have

$$s = m^2 + 2mE_1,$$
$$-t = Q^2 = 4E_1E_2\sin^2(\theta_e/2),$$
$$u = m^2 - 2mE_2,$$

where θ_e is the angle between the vectors $\boldsymbol{p}_1$ and $\boldsymbol{p}_2$, and $\cos(\theta_e) = \boldsymbol{p}_1\boldsymbol{p}_2/|\boldsymbol{p}_1||\boldsymbol{p}_2|$.

The energies of the final electron E_2 and the proton E_{2p} are related in the LF with $Q^2 = -q_-^2$ as follows:

$$E_2 = E_1 - Q^2/2m, \qquad E_{2p} = m + Q^2/2m. \tag{28}$$

For the dot products q_+^2, p_+q_+, and q_-^2, we have

$$q_+^2 = 4m^2 + 2mE_-, \qquad p_+q_+ = s - u = 2mE_+,$$
$$q_-^2 = -2mE_-, \qquad E_{2p} = m + E_-, \qquad E_\pm = E_1 \pm E_2. \tag{29}$$

The dependences of E_2 and Q^2 on the electron scattering angle θ_e in the LF are

$$E_2(\theta_e) = \frac{E_1}{1 + (2E_1/m)\sin^2(\theta_e/2)}, \tag{30}$$

$$Q^2(\theta_e) = \frac{4E_1^2\sin^2(\theta_e/2)}{1 + (2E_1/m)\sin^2(\theta_e/2)}. \tag{31}$$

The dependence of E_{2p} and Q^2 on the proton scattering angle θ_p has the form

$$E_{2p}(\theta_p) = m\frac{(E_1+m)^2 + E_1^2\cos^2(\theta_p)}{(E_1+m)^2 - E_1^2\cos^2(\theta_p)}, \tag{32}$$

$$Q^2(\theta_p) = \frac{4m^2E_1^2\cos^2(\theta_p)}{(E_1+m)^2 - E_1^2\cos^2(\theta_p)}, \tag{33}$$

where θ_p is the angle between the vectors $\boldsymbol{p}_1$ and $\boldsymbol{q}_2$, and $\cos(\theta_p) = \boldsymbol{p}_1\boldsymbol{q}_2/|\boldsymbol{p}_1||\boldsymbol{q}_2|$.

The inverse relations between θ_e, θ_p and E_2, E_{2p} can be written as

$$\theta_e = \arccos\left(1 - \frac{Q^2}{2E_1E_2}\right), \tag{34}$$

$$\theta_p = \arccos\left(\frac{E_1 + m}{E_1}\sqrt{\frac{\tau_p}{1+\tau_p}}\right). \tag{35}$$

In the elastic $ep \to ep$ process, the electron scattering angle θ_e changes from 0° to 180°, while Q^2 changes in the range of $0 \le Q^2 \le Q^2_{\max}$ $(0 \le \tau_p \le \tau_{\max})$, where

$$Q^2_{\max} = \frac{4ME_1^2}{(M+2E_1)}, \qquad \tau_{\max} = \frac{E_1^2}{M(M+2E_1)}. \tag{36}$$

Let us write the following useful relation:

$$\sqrt{\frac{\tau_{\max}}{1+\tau_{\max}}} = \frac{E_1}{M+E_1}. \tag{37}$$

According to Eq. (31), at $\theta_e = 0$ we have $Q^2 = 0$ and $\tau_p = 0$. However, from Eq. (35), it follows that in this case $\theta_p = 90°$. In the case of electron backscattering ($\theta_e = 180°$), when $\tau_p = \tau_{\max}$, it follows from Eqs. (35) and (37) that $\theta_p = 0°$. Thus, the electron scattering by an angle ranging from 0° to 180° ($0° \le \theta_e \le 180°$) leads to a change in the proton scattering angle from 90° to 0°.

The results of calculations of the dependence of the scattering angles of the electron θ_e and proton θ_p on the square of the momentum transferred to the proton Q^2 at electron beam energies $E_1 = 4.725$ GeV and 5.895 GeV in the SANE Collaboration experiment [17] are plotted in Fig. 1. They correspond to the lines labeled θ_{e4}, θ_{p4} and θ_{e5}, θ_{p5}.

The intersection points of the lines θ_{e4} and θ_{p4} (θ_{e5} and θ_{p5}) in Fig. 1 correspond to the equality $\theta_e = \theta_p$ for some values $Q^2 = Q^2_{(ep)}$. At the same time, $Q^2_{(ep)} = 3.70$ GeV^2 for $E_1 = 4.725$ GeV, and $Q^2_{(ep)} = 4.772$ GeV^2 for $E_1 = 5.895$ GeV. For the corresponding angles, we have $\theta_{ep} = 30.91°$ (0.54 rad) and $\theta_{ep} = 28.45°$ (0.50 rad).

The data on the electron and proton scattering angles (in radians) at electron beam energies $E_1 = 4.725$ and 5.895 GeV and $Q^2 = 2.06$ and 5.66 GeV^2 are represented in Table I, which contains also the values of $Q^2_{\max}$ [Eq. (36)] for the maximally possible Q^2 values at $E_1 = 4.725$ and 5.895 GeV.

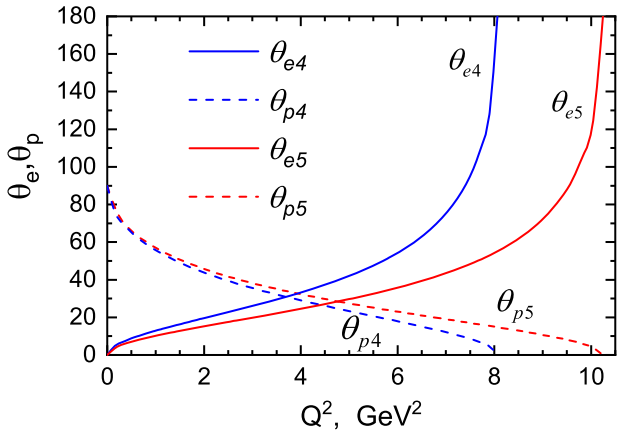

FIG. 1. Q^2 dependence of the scattering angles of the electron θ_e and the proton θ_p (in degrees) at electron beam energies in the experiment [17]. The lines θ_{e4}, θ_{p4} (θ_{e5}, θ_{p5}) correspond to $E_1 = 4.725$ (5.895) GeV.

IV. POLARIZATION OF A VIRTUAL PHOTON IN THE $ep \to ep$ PROCESS

The ε value entering into the expression for the Rosenbluth cross section [Eq. (1)] with the range of variation $0 \le \varepsilon \le 1$ in modern literature, as a rule, is identified not with the degree of linear (transverse) polarization, but with the degree of longitudinal polarization of the virtual photon. Sometimes it is also referred to as the polarization parameter, or simply the virtual photon polarization.

For example, in Ref. [53], ε in the massless case was interpreted as a degree of the longitudinal polarization in the OPE approximation. Similar statements have been made in a number of other works [9,12,14,16,22].

The correct understanding of the physical meaning of the value ε is quite rare [54–56], but recently the number of such works has gradually increased—see, for example, Refs. [57–59].

The most common expression in the literature for ε, given on the first page, actually contains the dependence on the electron scattering angle θ_e in the LF. Expressions for ε that make it possible to calculate the dependences of the quantities of interest on, e.g., Q^2 or the proton scattering angle θ_p, are given by

TABLE I. Electron and proton scattering angles θ_e and θ_p (in radians) in the kinematics of the experiment [17].

E_1 (GeV)	Q^2 (GeV^2)	θ_e (rad)	θ_p (rad)	$Q^2_{\max}$ (GeV)^2
5.895	2.06	0.27	0.79	10.247
5.895	5.66	0.59	0.43	10.247
4.725	2.06	0.35	0.76	8.066
4.725	5.66	0.86	0.35	8.066

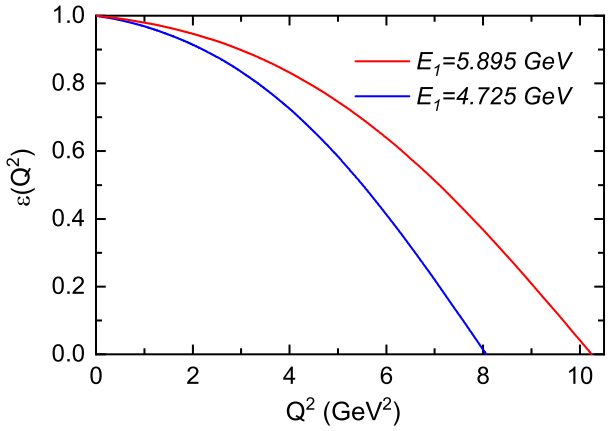

FIG. 2. Q^2 dependence of the degree of the linear polarization of the virtual photon, ε [Eq. (38)], for the electron beam energies used in the experiment [17].

$$\varepsilon^{-1} = 1 + \frac{(E_1 - E_2)^2 + 2(E_1 - E_2)m}{2E_1E_2 - (E_1 - E_2)m} = \frac{E_1^2 + E_2^2 + (E_1 - E_2)m}{2E_1E_2 - (E_1 - E_2)m}, \tag{38}$$

where E_1 and E_2 are the energies of the initial and final electrons, respectively. Note that Eq. (28) should be used for E_2; it depends explicitly only on Q^2. In turn, the Q^2 dependence on the angles θ_e or θ_p is determined by Eqs. (31) or (33).

The Q^2 dependence of the degree of the linear polarization of the virtual photon, ε [Eq. (38)], at electron beam energies in the SANE Collaboration experiment [17] is represented by graphs in Fig. 2.

Figure 3 shows the dependence of the degree of the linear polarization of the virtual photon, ε [Eq. (38)], on the scattering angles of the electron θ_e [Fig. 3(a)] and proton θ_p [Fig. 3(b)] for the electron beam energies $E_1 = 4.725$ and 5.895 GeV in the experiment [17].

It follows from Fig. 2 that ε is a function of Q^2 and decreases from 1 to 0. It follows from Fig. 3(a) that in the case of an electron scattered forward ($\theta_e = 0°$) when $Q^2 = 0$, $\varepsilon = 1$. For a backscattered electron ($\theta_e = 180°$) when $Q^2 = Q^2_{\max}$, $\varepsilon = 0$.

The $Q^2_{\max}$ values for the energies $E_1 = 4.725$ and 5.895 GeV are listed in Table I; they amount to 8.066 and 10.247 GeV^2, respectively. Specifically at these points, the lines in Fig. 2 intersect the abscissa axis.

V. POLARIZATION EFFECTS IN THE $e\vec{p} \to \vec{e}p$ PROCESS

A. Differential cross section of the $e\vec{p} \to \vec{e}p$ process

In the OPE approximation, the matrix elements of the process $ep \to ep$ are the product of the electron (J_e) and

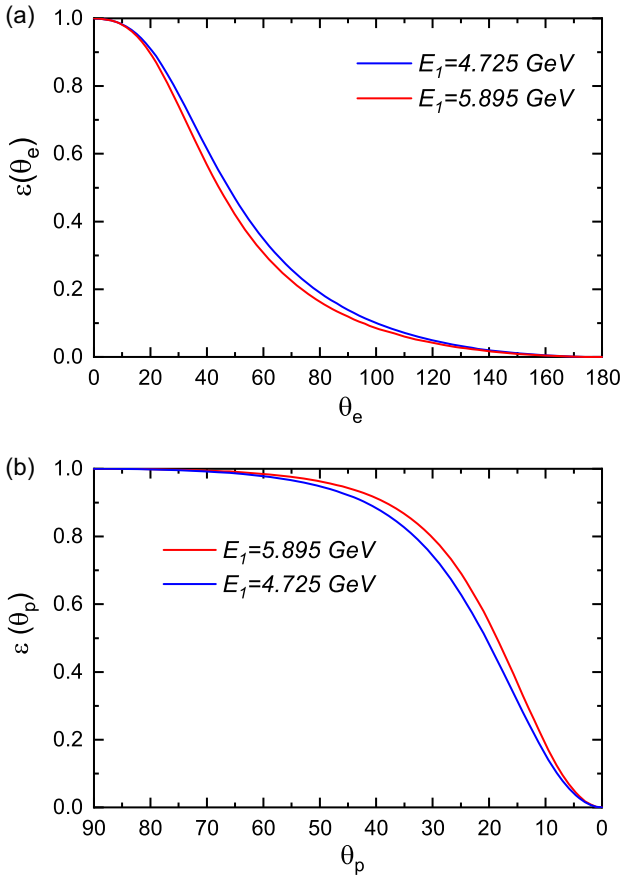

FIG. 3. Angular dependence of the degree of the linear polarization of the virtual photon, ε [Eq. (38)], on the scattering angles of (a) the electron θ_e and (b) the proton θ_p expressed in degrees for the electron beam energies in the experiment [17].

proton currents (J_p)

$$M_{ep\to ep} = 4\pi\alpha T_{ep}/q^2, \tag{39}$$

$$T_{ep} = (J_e)^\mu (J_p)_\mu. \tag{40}$$

The lepton $(J_e)^\mu$ and proton $(J_p)_\mu$ currents read

$$(J_e)^\mu = \bar{u}(p_2)\gamma^\mu u(p_1),$$
$$(J_p)_\mu = \bar{u}(q_2)\Gamma_\mu(q^2)u(q_1),$$
$$\Gamma_\mu(q^2) = F_1\gamma_\mu + \frac{F_2}{4m}(\hat{q}\gamma_\mu - \gamma_\mu\hat{q}).$$

Here, $u(p_i)$ and $u(q_i)$ are the bispinors of electrons and protons with the 4-momenta p_i and q_i, respectively, where $p_i^2 = m_0^2$ and $q_i^2 = m^2$, having the properties $\bar{u}(p_i)u(p_i) = 2m_0$ and $\bar{u}(q_i)u(q_i) = 2m$ $(i = 1, 2)$; F_1 and F_2 are the Dirac and Pauli proton form factors, respectively; $q = q_- = q_2 - q_1$ is the 4-momentum transferred to the proton; and $\hat{q} = (q)_\mu\gamma^\mu$, where γ^μ are the Dirac matrices.

It is well known that the SFFs G_E and G_M could be expressed in terms of the Dirac and Pauli proton form factors:

$$G_E = F_1 - \tau_p F_2, \qquad G_M = F_1 + F_2.$$

The differential cross section of the process $ep \to ep$ reads

$$\frac{d\sigma_{ep\to ep}}{dt} = \frac{\pi\alpha^2}{\lambda_s}\frac{|T_{ep}|^2}{t^2}, \tag{41}$$

where $\lambda_s = (s-(m+m_0)^2)(s-(m-m_0)^2)$ is Källén's function.

In the standard approach [49,50], the calculation of the squares of the amplitude modules $|T_{ep}|^2$ is reduced to the convolution of the lepton ($L^{\mu\nu}$) and hadron ($H_{\mu\nu}$) tensors:

$$|T_{ep}|^2 = H_{\mu\nu}L^{\mu\nu},$$

where

$$L^{\mu\nu} = \mathrm{Tr}(\tau_{e_2}\gamma^\mu\tau_{e_1}\gamma^\nu), \tag{42}$$

$$H_{\mu\nu} = 2\mathrm{Tr}(\tau_{p_2}\Gamma_\mu\tau_{p_1}\bar{\Gamma}_\nu). \tag{43}$$

Here, the symbol "Tr" denotes the operation to calculate the trace from Dirac's operators, while τ_{e_i} and τ_{p_i} $(i=1,2)$ are the polarization density matrices of the initial and final states of electrons and protons (λ_{p_1} and λ_{e_2} are the degrees of polarization of the initial proton and the final electron, and γ_5 is the Dirac matrix):

$$\begin{aligned}
\tau_{e_1} &= (\hat{p}_1 + m_0)/2,\\
\tau_{e_2} &= (\hat{p}_2 + m_0)(1-\lambda_{e_2}\gamma_5\hat{s}_{e_2})/2,\\
\tau_{p_1} &= (\hat{q}_1 + m)(1-\lambda_{p_1}\gamma_5\hat{s}_{p_1})/2,\\
\tau_{p_2} &= (\hat{q}_2 + m)/2.
\end{aligned} \tag{44}$$

The lepton tensor $L^{\mu\nu}$ [Eq. (42)] in terms of the 4-vectors $p_\pm$ has the form

$$2L^{\mu\nu} = p_+^\mu p_+^\nu - p_-^\mu p_-^\nu + p_-^2 g^{\mu\nu} + 2im_0\lambda_{e_2}\varepsilon^{\mu\nu\rho\sigma}(p_-)_\rho(s_{e_2})_\sigma.$$

In the ultrarelativistic limit, when $s_{e_2} = p_2/m_0$, it takes the form

$$2L^{\mu\nu} = p_+^\mu p_+^\nu - p_-^\mu p_-^\nu + p_-^2 g^{\mu\nu} + i\lambda_{e_2}\varepsilon^{\mu\nu\rho\sigma}(p_-)_\rho(p_+)_\sigma.$$

The explicit form of the tensor $H_{\mu\nu}$ [Eq. (43)] is rather cumbersome; for this reason, we omit it.

The expression for $|T_{ep}|^2$ can be written as

$$2|T_{ep}|^2 = \frac{4m^2}{q_+^2}|T|^2.$$

Since $q_+^2 = 4m^2(1+\tau_p)$, the differential cross section of the process (10) calculated in an arbitrary reference frame in the DSB (12) takes the form

$$\frac{d\sigma_{e\vec{p}\to\vec{e}p}}{dt} = \frac{\pi\alpha^2}{2\lambda_s(1+\tau_p)}\frac{|T|^2}{t^2}, \tag{45}$$

$$\begin{aligned}
|T|^2 &= I_0 + \lambda_{p_1}\lambda_{e_2}I_1,\\
I_0 &= G_E^2 Y_1 + \tau_p G_M^2 Y_2,\\
I_1 &= \tau_p(G_E G_M Y_3 + G_M^2 Y_4),
\end{aligned} \tag{46}$$

where λ_{p_1} and λ_{e_2} are the degrees of polarization of the initial proton and the final electron; the functions Y_i $(i=1,\ldots 4)$ are given by

$$\begin{aligned}
Y_1 &= (p_+q_+)^2 + q_+^2 q_-^2,\\
Y_2 &= (p_+q_+)^2 - q_+^2(q_-^2 + 4m_0^2),\\
-Y_3 &= 2\kappa_1 m^2((p_+q_+)^2 + q_+^2(q_-^2 - 4m_0^2))z_1^2,\\
Y_4 &= 2(m^2 p_+q_+ - \kappa_1 q_+^2)(\kappa_1 p_+q_+ - m_0^2 q_+^2)z_1^2,\\
z_1 &= (\kappa_1^2 - m^2 m_0^2)^{-1/2}, \qquad \kappa_1 = q_1 p_2.
\end{aligned} \tag{47}$$

In the case of arbitrary spin 4-vectors s_{p_1} and s_{e_2}, the expressions for Y_3 and Y_4 in the cross section (45) are given by

$$\begin{aligned}
Y_3 &= 8m_0 m(s_{p_1})^\mu (g^\perp)_{\mu\nu}(s_{e_2})^\nu q_+^2,\\
Y_4 &= 8m_0 m(q_+s_{p_1})(q_+s_{e_2}).
\end{aligned} \tag{48}$$

Note, first, that the polarized part of the cross section (45) includes the term with Y_3 containing the product of the SFFs, $G_E G_M$, and according to Eq. (48), it is determined by the transverse part of the metric tensor $(g^\perp)_{\mu\nu}$ [Eq. (25)]. Second, in the cross section of the process $e\vec{p} \to e\vec{p}$ in DSB [Eq. (6)], there is no similar structure; see Refs. [34–36].

In the ultrarelativistic limit, when the mass of an electron can be neglected, for the functions Y_i [Eq. (47)] in the LF, we obtain expressions that depend only on the energy of the initial and final electrons:

$$\begin{aligned}
Y_1 &= 8m^2(2E_1E_2 - mE_-),\\
Y_2 &= 8m^2(E_1^2 + E_2^2 + mE_-),\\
Y_3 &= -(2m/E_2)Y_1,\\
Y_4 &= 8m^2 E_+E_-(m-E_2)/E_2.
\end{aligned} \tag{49}$$

B. Polarization of the final electron in the $e\vec{p} \to \vec{e}p$ process

The expression for the square of the amplitude modulus $|T|^2$ [Eq. (46)] can be written as

$$|T|^2 = I_0 + \lambda_{p_1}\lambda_{e_2} I_1 = I_0(1 + \lambda_{e_2}\lambda^f_{e_2}), \tag{50}$$

where $\lambda^f_{e_2}$ is the degree of longitudinal polarization transferred from the initial proton to the final electron in the $e\vec{p} \to \vec{e}p$ process:

$$\lambda^f_{e_2} = \lambda_{p_1}\frac{I_1}{I_0} = \lambda_{p_1}\frac{\tau_p(G_E G_M Y_3 + G_M^2 Y_4)}{G_E^2 Y_1 + \tau_p G_M^2 Y_2}.$$

Dividing the numerator and denominator in the last expression by $Y_1 G_M^2$ and introducing the experimentally measured ratio $R \equiv \mu_p G_E/G_M$, we get

$$\lambda^f_{e_2} = \lambda_{p_1}\frac{\mu_p\tau_p((Y_3/Y_1)R + \mu_p(Y_4/Y_1))}{R^2 + \mu_p^2\tau_p(Y_2/Y_1)}. \tag{51}$$

Note that for the ratio Y_2/Y_1 in the denominator of Eq. (51) in the LF, the equality $Y_2/Y_1 = 1/\varepsilon$ is valid, where ε is the degree of linear polarization of the virtual photon (38).

Inverting relation (51), we obtain a quadratic equation with respect to R:

$$\alpha_0 R^2 - \alpha_1 R + \alpha_0\alpha_3 - \alpha_2 = 0, \tag{52}$$

with the coefficients

$$\alpha_0 = \lambda^f_{e_2}/\lambda_{p_1}, \qquad \alpha_1 = \tau_p\mu_p Y_3/Y_1,$$
$$\alpha_2 = \tau_p\mu_p^2 Y_4/Y_1, \qquad \alpha_3 = \tau_p\mu_p^2 Y_2/Y_1.$$

Solutions to Eq. (52) read

$$R = \frac{\alpha_1 \pm \sqrt{\alpha_1^2 - 4\alpha_0(\alpha_0\alpha_3 - \alpha_2)}}{2\alpha_0}.$$

They allow us to extract the ratio R from the results of an experiment to measure the polarization transferred to the electron $\lambda^f_{e_2}$ in the $e\vec{p} \to \vec{e}p$ process.

C. Results of numerical calculations of polarization effects

Equation (49) was used to numerically calculate the Q^2 dependence of the longitudinal polarization degree of the scattered electron $\lambda^f_{e_2}$ [Eq. (51)], as well as the dependence on the scattering angles of the electron and proton at electron beam energies ($E_1 = 4.725$ and 5.895 GeV) and the polarization degree of the proton target at rest ($\lambda_{p_1} = P_t = 0.70$) in the experiment [17], while conserving the scaling of the SFFs in the case of a dipole dependence

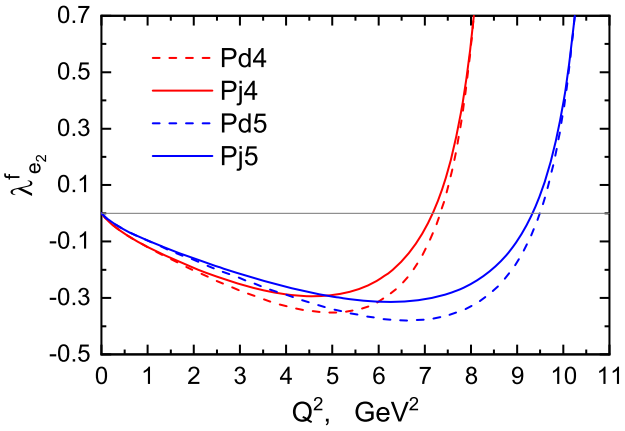

FIG. 4. Q^2 dependence of the longitudinal polarization degree of the scattered electron $\lambda^f_{e_2}$ [Eq. (51)] at electron beam energies in the experiment [17]. The lines $Pd4$, $Pd5$ (dashed) and $Pj4$, $Pj5$ (solid) correspond to the ratios $R = R_d$ and $R = R_j$ [Eq. (53)]. The lines $Pd4$, $Pj4$ ($Pd5$, $Pj5$) correspond to the energies $E_1 = 4.725$ (5.895) GeV.

$R = R_d$ ($R_d = 1$), and in the case of its violation. In the latter case, the parametrization $R = R_j$,

$$R_j = (1 + 0.1430Q^2 - 0.0086Q^4 + 0.0072Q^6)^{-1} \tag{53}$$

from Ref. [38] was used, and also the Kelly parametrization ($R = R_k$) from the Ref. [37] formulas which we omit.

The calculation results are presented by graphs in Figs. 4 and 5. Note that in these figures, there are no lines corresponding to the parametrization [37], since calculations using R_j and R_k give almost identical results.

The Q^2 dependence of the longitudinal polarization degree of the scattered electron $\lambda^f_{e_2}$ [Eq. (51)] is plotted in Fig. 4, on which the lines $Pd4$, $Pd5$ (dashed) and $Pj4$, $Pj5$ (solid) are constructed for $R = R_d$ and $R = R_j$ [Eq. (53)]. At the same time, the red lines $Pd4$, $Pj4$ and the blue lines $Pd5$, $Pj5$ correspond to the energy of the electron beam $E_1 = 4.725$ and 5.895 GeV. For all lines in Fig. 4, the degree of polarization of the proton target at rest $P_t = 0.70$.

As can be seen from the graphs in Fig. 4, the function $\lambda^f_{e_2}(Q^2)$ [Eq. (51)] takes negative values for most of the allowed values Q^2 and has a minimum for some of them. We will specify them: $Pd4(4.976) = -0.352$, $Pj4(4.586) = -0.294$, $Pd5(6.648) = -0.380$, and $Pj5(6.254) = -0.314$. We also give the values for Q^2, at which the lines in Fig. 4 intersect with the abscissa axis (begin to take positive values): $Pj4(7.174) = 0$, $Pd4(7.340) = 0$, $5(9.333) = 0$, and $Pd5(9.492) = 0$. Thus, in a smaller part of the allowed values adjacent to $Q^2_{\max}$ and amounting to approximately 9% of $Q^2_{\max}$, the function $\lambda^f_{e_2}(Q^2)$ takes positive values. At the boundary of the spectrum at $Q^2 = Q^2_{\max}$, the polarization

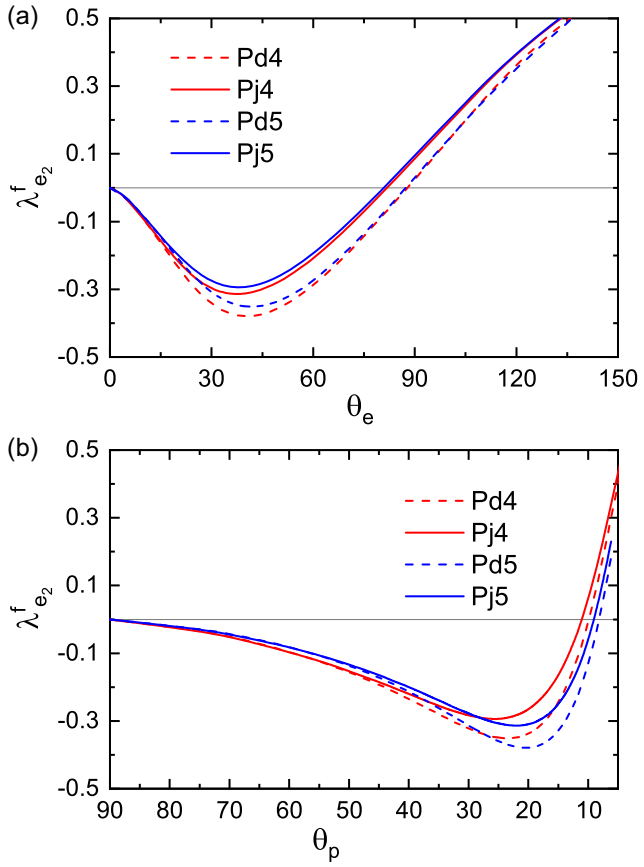

FIG. 5. Angular dependence of the degree of the transferred polarization to the electron polarization $\lambda^f_{e_2}$ [Eq. (51)] at electron beam energies used in the experiment [17] on the scattering angle (a) of the electron θ_e and (b) of the proton θ_p, expressed in degrees. The marking of lines $Pd4$, $Pd5$, $Pj4$, $Pj5$ is the same as in Fig. 4.

transferred to the electron is equal to the polarization of the proton target, $\lambda^f_{e_2}(Q^2_{\max}) = P_t = 0.70$.

The results of calculations of the angular dependence of the polarization transferred to the electron $\lambda^f_{e_2}$ [Eq. (51)] in the $e\vec{p} \to \vec{e}p$ process at electron beam energies $E_1 = 4.725$ GeV and $E_1 = 5.895$ GeV in the experiment [17] as functions of the scattering angles of the electron (θ_e) and proton (θ_p) are represented by graphs in Fig. 5. The degree of polarization of the proton target for all lines was taken to be the same and equal to $P_t = 0.70$. Figures 5(a) and 5(b) represent the dependence on the scattering angles of the electron θ_e and proton θ_p, respectively.

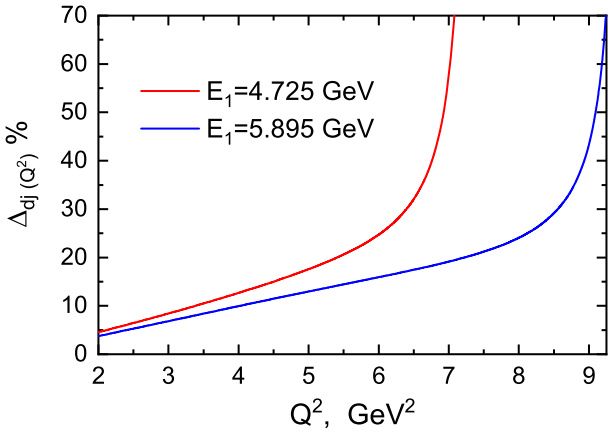

FIG. 6. Q^2 dependence of the relative difference Δ_{dj} [Eq. (54)] at electron beam energies $E_1 = 4.725$ GeV (red line) and $E_1 = 5.895$ GeV (blue line). For all lines, the degree of polarization of the proton target was taken to be the same, $P_t = 0.70$.

Obviously, the behavior of the lines in Fig. 5 for the angular dependence is similar to the behavior of the lines for the Q^2 dependence in Fig. 4.

Using the Kelly [37] and Qattan [38] parametrizations, the relative difference Δ_{dj} between the polarization effects in the process of $e\vec{p} \to \vec{e}p$ was calculated in the cases of conservation and violation of the scaling of the SFFs, as well as in the effects between these parametrizations Δ_{jk}:

$$\Delta_{dj} = \left|\frac{\mathrm{Pd} - \mathrm{Pj}}{\mathrm{Pd}}\right|, \qquad \Delta_{jk} = \left|\frac{\mathrm{Pj} - \mathrm{Pk}}{\mathrm{Pj}}\right|, \tag{54}$$

where P_d, P_j, and P_k are the polarizations calculated by formula (51) for $\lambda^f_{e_2}$ when using the corresponding parametrizations R_d, R_j, and R_k. The results of calculations of Δ_{dj} at electron beam energies of 4.725 and 5.895 GeV are shown in Fig. 6.

It follows from the graphs in Fig. 6 that the relative difference between the polarization transferred from the initial proton to the final electron in the $e\vec{p} \to \vec{e}p$ process in the cases of conservation and violation of the scaling of the

TABLE II. The degree of longitudinal polarization of the scattered electron $\lambda^f_{e_2}$ [Eq. (51)] at E_1 and Q^2 used in the experiment [17]. The values in the columns for P_d, P_j, and P_k correspond to dipole dependence and the Qattan [38] and Kelly [37] parametrizations [Eq. (53)]. The corresponding electron and proton scattering angles (in degrees) are given in columns for θ_e and θ_p.

E_1, GeV	Q^2, GeV^2	$\theta_e(^\circ)$	$\theta_p(^\circ)$	P_d	P_j	P_k	Δ_{dj}, %	Δ_{jk}, %
5.895	2.06	15.51	45.23	−0.170	−0.163	−0.163	4.1	0.0
5.895	5.66	33.57	24.48	−0.363	−0.309	−0.308	14.9	0.3
4.725	2.06	19.97	43.27	−0.207	−0.197	−0.197	4.8	0.0
4.725	5.66	49.50	19.77	−0.336	−0.263	−0.262	21.7	0.6

SFFs can reach 70%, which can be used to set up a polarization experiment by measuring the ratio R.

Numerical values of the polarization transferred to the final electron in the $e\vec{p} \to \vec{e}p$ process for the three considered parametrizations of the ratio R at E_1 and Q^2 used in the experiment [17] are represented in Table II. In it, the columns of values P_d, P_j, and P_k correspond to the dipole dependence R_d, the parametrizations R_j [Eq. (53)] from Ref. [38], and R_k [37]; the columns Δ_{dj}, Δ_{jk} correspond to the relative difference [Eq. (54)] (expressed in percent) at electron beam energies of 4.725 and 5.895 GeV and two values of Q^2 equal to 2.06 and 5.66 GeV^2. It follows from Table II that the relative difference between $Pj5$ and $Pd5$ at $Q^2 = 2.06$ GeV^2 is 4.1%, and between $Pj4$ and $Pd4$ it is 4.8%. At $Q^2 = 5.66$ GeV^2, these differences increase and become equal to 14.9% and 21.7%, respectively. Note that the relative difference Δ_{jk} between P_j and P_k for all E_1 and Q^2 in Table II is less than 1%.

VI. POLARIZATION EFFECTS IN THE $\vec{e}\vec{p} \to ep$ PROCESS

In the OPE approximation, the differential cross section of the process (16), calculated in an arbitrary reference frame in DSB [Eq. (18)], reads

$$\frac{d\sigma_{\vec{e}\vec{p}\to ep}}{dt} = \frac{\pi\alpha^2}{\lambda_s(1+\tau_p)}\frac{|T|^2}{t^2}, \tag{55}$$

$$\begin{aligned} |T|^2 &= I_0 + \lambda_{e_1}\lambda_{p_1} I_1, \\ I_0 &= G_E^2 Y_1 + \tau_p G_M^2 Y_2, \\ I_1 &= \tau_p (G_E G_M Y_3 + G_M^2 Y_4), \end{aligned} \tag{56}$$

where λ_{e_1} and λ_{p_1} are the degrees of polarization of the initial electron and proton, and the functions Y_i $(i = 1, \ldots 4)$ read

$$\begin{aligned} Y_1 &= (p_+q_+)^2 + q_+^2 q_-^2, \\ Y_2 &= (p_+q_+)^2 - q_+^2(q_-^2 + 4m_0^2), \\ -Y_3 &= 2\kappa_2 m^2((p_+q_+)^2 + q_+^2(q_-^2 - 4m_0^2))z_2^2, \\ Y_4 &= 2(m^2 p_+q_+ - \kappa_2 q_+^2)(\kappa_2 p_+q_+ - m_0^2 q_+^2)z_2^2, \\ z_2 &= (\kappa_2^2 - m^2 m_0^2)^{-1/2}, \qquad \kappa_2 = q_1 p_1. \end{aligned} \tag{57}$$

In the case of arbitrary spin 4-vectors s_{e_1} and s_{p_1}, the expressions for Y_3 and Y_4 in the cross section (55) have the form

$$\begin{aligned} Y_3 &= 8m_0 m (s_{p_1})^\mu (g^\perp)_{\mu\nu} (s_{e_1})^\nu q_+^2, \\ Y_4 &= 8m_0 m (q_+ s_{p_1})(q_+ s_{e_1}). \end{aligned} \tag{58}$$

Note, first, that the polarized part of the cross section (55) includes the term with Y_3 containing the product of the SFFs, $G_E G_M$, and according to Eq. (58), is determined by the transverse part of the metric tensor $(g^\perp)_{\mu\nu}$ [Eq. (25)]. Second, there is no similar structure in the cross section of the $e\vec{p} \to \vec{e}p$ process in the DSB [Eq. (6)]; see Refs. [34–36].

In the ultrarelativistic limit, when the mass of an electron can be neglected, for the functions Y_i [Eq. (57)] in the LF, we obtain expressions that depend only on the energy of the initial and final electrons:

$$\begin{aligned} Y_1 &= 8m^2(2E_1E_2 - mE_-), \\ Y_2 &= 8m^2(E_1^2 + E_2^2 + mE_-), \\ -Y_3 &= (2m/E_1)Y_1, \\ -Y_4 &= 8m^2 E_+ E_- (m + E_1)/E_1. \end{aligned} \tag{59}$$

The polarization asymmetry in the process (16) is determined by the square of the amplitude modulus (56) as follows [55,56]:

$$A = \frac{|T|^2(\lambda_{e_1} = -1) - |T|^2(\lambda_{e_1} = +1)}{|T|^2(\lambda_{e_1} = -1) + |T|^2(\lambda_{e_1} = +1)}.$$

As a result, we have

$$A = -\lambda_{p_1}\frac{\tau_p(G_E G_M Y_3 + G_M^2 Y_4)}{G_E^2 Y_1 + \tau_p G_M^2 Y_2}.$$

By dividing the numerator and denominator in the last expression into $Y_1 G_M^2$ and introducing the experimentally measured ratio $R \equiv \mu_p G_E/G_M$, we get

$$A = -\lambda_{p_1}\frac{\mu_p\tau_p((Y_3/Y_1)R + \mu_p(Y_4/Y_1))}{R^2 + \mu_p^2\tau_p(Y_2/Y_1)}. \tag{60}$$

Note that Eq. (60) for polarization asymmetry in the $\vec{e}\,\vec{p} \to ep$ process and Eq. (51) for electron transferred polarization $\lambda_{e_2}^f$ in the $e\vec{p} \to \vec{e}p$ process coincide up to the sign. For this reason, the quadratic equation for extracting the ratio R coincides with the explicit form of Eq. (52) and has coefficients of the same shape, except for one: $\alpha_0 = -A_{\rm exp}/\lambda_{p_1}$, where $A_{\rm exp}$ is the experimentally measured polarization asymmetry.

The results of numerical calculations of the Q^2 dependence of the polarization asymmetry A [Eq. (60)] in the $\vec{e}\,\vec{p} \to ep$ process at electron beam energies $E_1 = 4.725$ and 5.895 GeV are represented by graphs in Fig. 7, from which it follows that this dependence for each of the energies of the electron beam is almost linear. With the increase of Q^2 from 0 to $Q^2_{\rm max}$, it changes from 0 to $P_t = 0.70$ at the boundaries of the spectrum at $Q^2 = Q^2_{\rm max}$. The effects of scaling violations are small in the entire range of

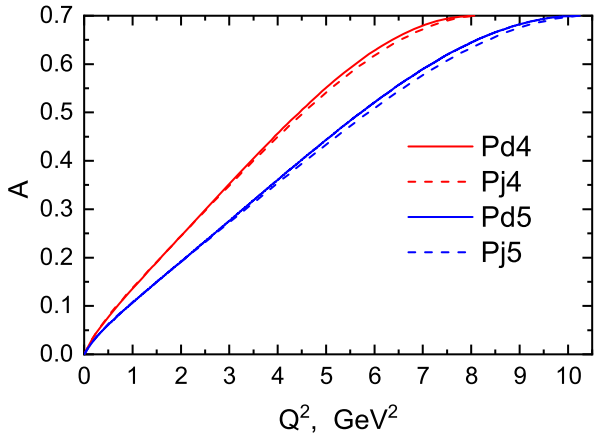

FIG. 7. Q^2 dependence of the polarization asymmetry of A [Eq. (60)] in the $\vec{e}\,\vec{p} \to ep$ process at electron beam energies in the experiment [17]. The lines $Pd4, Pd5$ (solid) and $Pj4$, $Pj5$ (dashed) correspond to the dipole dependence $R = R_d$ ($R_d = 1$) and parametrization of $R = R_j$ [Eq. (53)] from Ref. [38]. The lines $Pd4, Pj4$ ($Pd5, Pj5$) correspond to the electron beam energy 4.725 and 5.895 GeV. For all lines, the degree of polarization of the proton target was taken to be the same, $P_t = 0.70$.

acceptable values of Q^2; they do not exceed 1.79% at $E_1 = 4.725$ GeV or 2.32% at $E_1 = 5.895$ GeV. For this reason, the measurement of polarization asymmetry in the $\vec{e}\,\vec{p} \to ep$ process can be used as a test to verify the conservation of the SFF scaling.

Note that the double-spin asymmetry in the elastic process $\vec{e}\,\vec{p} \to ep$ in the case when the spin quantization axes of a resting proton target and an incident electron beam are parallel was first measured in the experiment [55], as a result of which it was first established that the SFF ratio R is positive.

VII. CONCLUSION

In this paper, in the one-photon exchange approximation, we analyze polarization effects in the elastic $\vec{e}\,\vec{p} \to ep$ and $e\vec{p} \to \vec{e}p$ processes in the case when the spin quantization axes of the target proton at rest and the incident or scattered electron are parallel. To do this, in the kinematics of the SANE Collaboration experiment [17] using the Kelly [37] and Qattan [38] parametrizations for the Sachs form-factor ratio $R \equiv \mu_p G_E/G_M$, a numerical analysis was carried out of the dependence of the longitudinal polarization degree transferred to the scattered electron in the $e\vec{p} \to \vec{e}p$ process and the double-spin asymmetry in the $\vec{e}\,\vec{p} \to ep$ process on the square of the momentum transferred to the proton, as well as on the scattering angle of the electron. As it turned out, the Kelly [37] and Qattan [38] parametrizations give almost identical results.

As a result of calculations, it was established that the relative difference in the longitudinal polarization degree of the final electron in the $e\vec{p} \to \vec{e}p$ process for the case of conservation and violation of the SFF scaling can reach 70%, which can be used to conduct a polarization experiment of a new type of measurement of the SFF ratio R.

For the double-spin asymmetry in the $\vec{e}\,\vec{p} \to ep$ process, this difference is rather small and does not exceed 1.79% for the electron beam energy $E_1 = 4.725$ GeV or 2.32% for $E_1 = 5.895$ GeV. For this reason, the measurement of polarization asymmetry in the $\vec{e}\,\vec{p} \to ep$ process can be used as a test to verify the conservation of the SFF scaling.

At present, the experiment on measuring the degree of longitudinal polarization transferred to the final electron in the process $e\vec{p} \to \vec{e}p$ seems to be quite realistic, since a proton target with a high degree of polarization $P_t = 70 \pm 5\%$ has been already created and is used in the experiment [17]. For this reason, it would be most appropriate to conduct the proposed experiment at the setup used in Ref. [17] at the same proton polarization degree, $P_t = 0.70$, with electron beam energies $E_1 = 4.725$ and 5.895 GeV.

The difference between the proposed experiment and the one in [17] consists in the fact that an incident electron beam must be unpolarized, and the detected scattered electron must move strictly along the direction of the spin quantization axis of a resting proton target. In the proposed experiment, it is necessary to measure only the longitudinal polarization degree of the scattered electron, which is an advantage compared to the AR method [4] used in JLab polarization experiments.

ACKNOWLEDGMENTS

This work was carried out within the framework of the Belarus-JINR scientific cooperation and State Program of Scientific Research "Convergence-2025" of the Republic of Belarus under Projects No. 20241529 and No. 20210852.

[1] R. Hofstadter, F. Bumiller, and M. R. Yearian, Rev. Mod. Phys. **30**, 482 (1958).
[2] M. N. Rosenbluth, Phys. Rev. **79**, 615 (1950).
[3] N. Dombey, Rev. Mod. Phys. **41**, 236 (1969).
[4] A. I. Akhiezer and M. P. Rekalo, Fiz. Elem. Chastits At. Yadra **4**, 662 (1973) [Sov. J. Part. Nucl. **4**, 277 (1974)].
[5] A. I. Akhiezer and M. P. Rekalo, *Electrodynamics of Hadrons* (Naukova Dumka, Kiev, 1977) [in Russian].

[6] M. V. Galynskii and M. I. Levchuk, Yad. Fiz. **60**, 2028 (1997) [Phys. At. Nucl. **60**, 1855 (1997)].
[7] S. Pacetti, R. Baldini Ferroli, and E. Tomasi-Gustafsson, Phys. Rep. **550–551**, 1 (2015).
[8] Y. S. Liu and G. A. Miller, Phys. Rev. C **92**, 035209 (2015).
[9] M. K. Jones, K. A. Aniol, F. T. Baker *et al.*, Phys. Rev. Lett. **84**, 1398 (2000).
[10] O. Gayou, K. Wijesooriya, A. Afanasev *et al.*, Phys. Rev. C **64**, 038202 (2001).
[11] O. Gayou, K. A. Aniol, T. Averett *et al.*, Phys. Rev. Lett. **88**, 092301 (2002).
[12] V. Punjabi, C. F. Perdrisat, K. A. Aniol *et al.*, Phys. Rev. C **71**, 055202 (2005).
[13] A. J. R. Puckett, E. J. Brash, M. K. Jones *et al.*, Phys. Rev. Lett. **104**, 242301 (2010).
[14] A. J. R. Puckett, E. J. Brash, O. Gayou *et al.*, Phys. Rev. C **85**, 045203 (2012).
[15] A. J. R. Puckett, E. J. Brash, M. K. Jones *et al.*, Phys. Rev. C **96**, 055203 (2017).
[16] I. A. Qattan, J. Arrington, R. E. Segel *et al.*, Phys. Rev. Lett. **94**, 142301 (2005).
[17] A. Liyanage *et al.* (SANE Collaboration), Phys. Rev. C **101**, 035206 (2020).
[18] T. W. Donnelly and A. S. Raskin, Ann. Phys. (N.Y.) **169**, 247 (1986).
[19] J. C. Bernauer *et al.*, Phys. Rev. Lett. **105**, 242001 (2010).
[20] J. C. Bernauer *et al.*, Phys. Rev. C **90**, 015206 (2014).
[21] J. C. Bernauer, Ph.D. thesis, Mainz Universitat, Institute for Kernphysics, 2010, http://inspirehep.net/record/1358265/.
[22] J. Arrington, P. G. Blunden, and W. Melnitchouk, Prog. Part. Nucl. Phys. **66**, 782 (2011).
[23] V. Punjabi, C. F. Perdrisat, M. K. Jones, E. J. Brash, and C. E. Carlson, Eur. Phys. J. A **51**, 79 (2015).
[24] A. Afanasev, P. G. Blunden, D. Hasell, and B. A. Raue, Prog. Part. Nucl. Phys. **95**, 245278 (2017).
[25] I. A. Rachek *et al.* (VEPP-3 Collaboration), Phys. Rev. Lett. **114**, 062005 (2015).
[26] B. S. Henderson *et al.* (OLYMPUS Collaboration), Phys. Rev. Lett. **118**, 092501 (2017).
[27] M. Moteabbed *et al.* (CLAS Collaboration), Phys. Rev. C **88**, 025210 (2013).
[28] D. Adikaram *et al.* (CLAS Collaboration), Phys. Rev. Lett. **114**, 062003 (2015).
[29] D. Rimal *et al.* (CLAS Collaboration), Phys. Rev. C **95**, 065201 (2017).
[30] R. Alarcon, R. Beck, J. C. Bernauer *et al.*, Eur. Phys. J. A **60**, 81 (2024).
[31] M. V. Galynskii, E. A. Kuraev, and Yu. M. Bystritskiy, JETP Lett. **88**, 481 (2008).
[32] M. V. Galynskii, JETP Lett. **109**, 1 (2019).
[33] M. V. Galynskii and R. E. Gerasimov, JETP Lett. **110**, 646 (2019).
[34] M. V. Galynskii, JETP Lett. **113**, 555 (2021).
[35] M. V. Galynskii, Phys. Part. Nucl. Lett. **19**, 26 (2022).
[36] M. V. Galynskii, JETP Lett. **116**, 420 (2022).
[37] J. J. Kelly, Phys. Rev. C **70**, 068202 (2004).
[38] I. A. Qattan, J. Arrington, and A. Alsaad, Phys. Rev. C **91**, 065203 (2015).
[39] M. V. Galynskii, Yu. M. Bystritskiy, and V. M. Galynsky, Phys. Rev. D **108**, 096032 (2023).
[40] E. J. Brash, A. Kozlov, S. Li, and G. M. Huber, Phys. Rev. C **65**, 051001 (2002).
[41] K. M. Graczyk, P. Plonski, and R. Sulej, J. High Energy Phys. 09 (2010) 053.
[42] R. S. Sufian, G. F. de Teramond, S. J. Brodsky, A. Deur, and H. G. Dosch, Phys. Rev. D **95**, 014011 (2017).
[43] W. M. Alberico, S. M. Bilenky, C. Giunti, and K. M. Graczyk, Phys. Rev. C **79**, 065204 (2009).
[44] Kaushik Borah, Richard J. Hill, Gabriel Lee, and Oleksandr Tomalak, Phys. Rev. D **102**, 074012 (2020).
[45] Z. Ye, J. Arrington, R. J. Hill, and G. Lee, Phys. Lett. B **777**, 8 (2018).
[46] M. Jacob and G. Wick, Ann. Phys. (N.Y.) **7**, 404 (1959).
[47] F. I. Fedorov, Theor. Math. Phys. **2**, 248 (1970).
[48] F. I. Fedorov, *The Lorentz Group* (Nauka, Moscow, 1979) [in Russian].
[49] A. I. Akhiezer and V. B. Berestetskii, *Quantum Electrodynamics*, 3rd ed. (Nauka, Moscow, 1969; Wiley, New York, 1965).
[50] V. B. Berestetskii, E. M. Lifshits, and L. P. Pitaevskii, *Course of Theoretical Physics*, Vol. 4: *Quantum Electrodynamics* (Nauka, Moscow, 1989; Pergamon, Oxford, 1982).
[51] S. M. Sikach, Vesti Akad. Nauk BSSR, Ser. Fiz. Mat. Nauk **2**, 84 (1984) [in Russian].
[52] M. V. Galynskii and S. M. Sikach, Fiz. Elem. Chastits At. Yadra **29**, 1133 (1998), http://www1.jinr.ru/Archive/Pepan/1998-v29/v-29-5/pdf_obzory/v29p5_03.pdf [Phys. Part. Nucl. **29**, 469 (1998)].
[53] O. Tomalak and M. Vanderhaeghen, Phys. Rev. D **90**, 013006 (2014).
[54] G. I. Gakh and E. Tomasi-Gustafsson, Nucl. Phys. **A799**, 127 (2008).
[55] M. J. Alguard *et al.*, Phys. Rev. Lett. **37**, 1258 (1976).
[56] M. J. Alguard *et al.*, Phys. Rev. Lett. **37**, 1261 (1976).
[57] O. Tomalak and M. Vanderhaeghen, Eur. Phys. J. C **78**, 514 (2018).
[58] N. Korchagin and A. Radzhabov, arXiv:2106.06883.
[59] F. Gil-Dominguez, J. Alarcon, and C. Weiss, Phys. Rev. D **108**, 074026 (2023).